

How to Use an Adaptive High-gain Observer in Diagnosis Problems

Frédéric Lafont^{1,2}, Jean-François Balmat¹, Nathalie Pessel^{1,2} and Jean-Paul Gauthier^{1,2}

¹Université du Sud-Toulon-Var, LSIS, UMR CNRS 7296, B.P 20132, 83957 La Garde Cedex, France

²Institut Universitaire de Technologie de Toulon, B.P 20132, 83957 La Garde Cedex, France

Keywords: Observer, Diagnosis, Sensor.

Abstract: This paper explains how to use an adaptive High-Gain observer in sensor diagnosis problems. This type of observer allows to switch between a classical Extended Kalman Filter and High-Gain observer according to an innovation function. Combined with a standard technique of residual generation, this approach is very efficient to determine fault occurrence in the non-linear dynamical systems. We present the obtained results on a wastewater treatment system.

1 INTRODUCTION

Nowadays, systems are more and more automated in order to reduce the human intervention. So, these systems are composed of sensors and actuators. Therefore, it involves to define a structure enable to detect a sensor fault or a failing actuator. The aim of such equipment is the diagnosis of failure to avoid the economic losses and/or the environmental risks.

The present work deals the sensor diagnosis with an observer for non-linear dynamical systems applied to a wastewater treatment system. There is a lot of works on the synthesis of non-linear observers for (bio)chemical processes (Alcaraz-Gonzalez et al., 2002; Assis and Filho, 2000; Dochain, 2008; Methnani et al., 2011; Nejari et al., 2008; Sotomayor et al., 2002). In this study, we choose an adaptive high-gain observer, developed already as software sensor (Boizot et al., 2010; Lafont et al., 2011), to solve a sensor diagnosis problem. Transition from High-Gain (HG) mode to Extended Kalman Filter (EKF) mode is performed via an adaptation procedure based upon the level of innovation. In the context of large transitions, the HG observer guarantees theoretical convergence with arbitrary rate, under certain observability assumptions. For small enough error of initial estimation, classical EKF is more or less optimal w.r.t. noise.

Usually a changing coordinates is necessary in order to obtain an observability canonical form. In some cases, this change of coordinates is very complicated. To avoid this step, we write our observer in the natural coordinates. However, the counterpart of this choice

is that the Riccati equation of the Kalman filter has not the standard form (Lafont et al., 2011).

A such observer is “robust” compared with initial conditions and measurement noises. Although the generation of residues is standard, we show the capability of adaptive HG-EKF observer to detect a sensor fault.

Section 2 summarizes sensor diagnosis problems and observer-based residual generation. In Section 3, we recall the structure of the adaptive high-gain observer, which is the multi-output version developed in the paper (Boizot et al., 2010). Also, the crucial concept of innovation, which is used in order to switch between the EKF and HG-EKF modes, is presented. Section 4 is devoted to the application: A wastewater treatment plant. Finally, in Section 5, we show simulation results.

2 SENSOR DIAGNOSIS AND OBSERVER

2.1 Sensor Diagnosis

We are interested at the problem of the bias and the drift faults. These two faults are the most common and the most repetitive.

An output with a bias fault is defined by:

$$y_i = y_r + b, \quad (1)$$

with y_i is the measured output, y_r the real output and b the constant offset value.

An output with a drift fault is defined by:

$$y_i = y_r + d(t), \tag{2}$$

with y_i is the measured output, y_r the real output and $d(t)$ the time varying offset factor. $d(t)$ can be represented by the function: $d(t) = a t + b$ with a and b two constant terms.

2.2 Observer-based Residual Generation

The main problem for the diagnosis based on observers is to find the residues. They are neglectable in the absence of fault and significantly affected when some faults occur. One difficulty is to make the robust observer w.r.t. disturbances which are no faults.

So, a non-linear system can be written:

$$\begin{aligned} \frac{dx}{dt} &= f(x, u), \\ y &= h(x) = Cx, \end{aligned} \tag{3}$$

where x is the state vector, y the measured outputs and u the control variables.

The corresponding observer is defined by:

$$\begin{aligned} \frac{d\hat{x}}{dt} &= g(\hat{x}, u), \\ \hat{y} &= \hat{C}\hat{x}, \end{aligned} \tag{4}$$

The output estimation error is used to residual generation. The residual is analysed to determine fault occurrence. We apply a standard method:

$$r_i = |y_i - \hat{y}_i|. \tag{5}$$

The output has a fault if $r_i > \delta_i$. For each output, we simulate off-line in nominal operating (without fault) to determine the threshold level δ_i . Then, the method is applied on-line.

3 SYSTEMS UNDER CONSIDERATION AND OBSERVER EQUATIONS

3.1 The Observability Canonical Form

We consider a smooth non-linear system of the form (3) which is mapped by a diffeomorphism ψ into the following system:

$$\begin{aligned} \frac{d\xi}{dt} &= F(\xi, u) = A(t)\xi + b(\xi, u), \\ y &= C\xi, \end{aligned} \tag{6}$$

where $\xi \in \mathbb{R}^n$ is the state vector in observable coordinates (n the system order), where u are the control variables belonging to a certain bounded subset of \mathbb{R}^p

(p the number of the control variables) and the output $y \in \mathbb{R}^{d_0}$ (d_0 the number of the outputs).

The matrices $A(t)$, C and the vector $b(\xi, u)$ have a following form (all details can be found in (Boizot et al., 2010)):

$$A(t) = \begin{pmatrix} 0 & a_2(t) & 0 & \dots & 0 \\ 0 & 0 & a_3(t) & \ddots & \vdots \\ \vdots & \dots & \ddots & \ddots & 0 \\ \vdots & \dots & \dots & 0 & a_k(t) \\ 0 & 0 & \dots & \dots & 0 \end{pmatrix}, \tag{7}$$

$$C = (a_1(t), 0, \dots, 0) = (Id, 0, \dots, 0),$$

where Id is an identity matrix of order d_0 .

$$b(\xi, u) = \begin{pmatrix} b_1(\xi_1, u) \\ b_2(\xi_1, \xi_2, u) \\ \vdots \\ b_n(\xi_1, \dots, \xi_k, u) \end{pmatrix}. \tag{8}$$

The state vector $\xi(t)$ is assumed to have a “block” structure $\xi = (\xi'_1 \xi'_2 \dots \xi'_k)'$, where $\xi_i \in \mathbb{R}^{d_i-1}$ (d_i the size of $i + 1^{th}$ “block”) with $d_0 \geq d_1 \geq \dots \geq d_{k-1}$. The matrices $a_i(t)$ have dimension $d_{i-1} \times d_i$ and belong to a compact subset K_i of the set of $d_{i-1} \times d_i$ matrices of maximum rank d_i .

The $f(x, u)$, $a_i(t)$ and $b_i(\xi, u)$ are assumed smooth w.r.t. ξ , u and t . The b_i depend on ξ in a “block” triangular way and are compactly supported.

3.2 Observer Structure

Let Q ($n \times n$), R ($d_0 \times d_0$) be symmetric positive definite matrices. Let θ be the high-gain parameter, $\theta \geq 1$. For $\theta = 1$ the observer will just be an ordinary EKF.

Set $\Delta = BD \left(1, \frac{1}{\theta}, \dots, \frac{1}{\theta^{k-1}} \right)$, the block diagonal matrix with diagonal blocks $Id_{d_0}, \frac{1}{\theta} Id_{d_1}, \dots$. Set $Q_\theta = \theta \Delta^{-1} Q \Delta^{-1}, R_\theta = \theta^{-1} R$.

The equations of the system in observable coordinates are:

$$\begin{aligned} \frac{d\xi}{dt} &= T\psi(\psi^{-1}(\xi)) f(\psi^{-1}(\xi), u), \\ \frac{d\xi}{dt} &= F(\xi, u). \end{aligned} \tag{9}$$

The equations for the HG-EKF in the observable coordinates are:

$$\frac{d\hat{\xi}}{dt} = F(\hat{\xi}, u) + PC'R_\theta^{-1}(y - C\hat{\xi}), \tag{10}$$

$$\begin{aligned} \frac{dP}{dt} &= TF(\hat{\xi}, u)P + PTF(\hat{\xi}, u)' + Q_\theta \\ &- PC'R_\theta^{-1}CP. \end{aligned} \tag{11}$$

In the natural coordinates we have $\hat{x} = \psi^{-1}(\hat{\xi}) = \Phi(\hat{x})$, where \hat{x} denotes the estimate of x . As shown in (Lafont et al., 2011), the equations for the HG-EKF become:

$$\frac{d\hat{x}}{dt} = f(\hat{x}, u) + pC'(\hat{x}, u)R_{\theta}^{-1}(y - h(\hat{x})), \quad (12)$$

$$\begin{aligned} \frac{dp}{dt} = & Tf(\hat{x}, u)p + pTf(\hat{x}, u)' + q_{\theta}(\hat{x}) \\ & - pC'R_{\theta}^{-1}Cp \\ & + T\Psi(\hat{x})^{-1}D^2\Psi(\hat{x})\left\{pC'R_{\theta}^{-1}(h(\hat{x}) - y)\right\}p \\ & + pD^2\Psi(\hat{x})\left\{pC'R_{\theta}^{-1}(h(\hat{x}) - y)\right\}'\left(T\Psi(\hat{x})^{-1}\right)', \end{aligned} \quad (13)$$

where

$$p = T\Phi\left(\hat{\xi}\right)P T\Phi\left(\hat{\xi}\right)' \quad (14)$$

and

$$q_{\theta}(\hat{x}) = (T\Psi(\hat{x}))^{-1}Q_{\theta}\left((T\Psi(\hat{x}))^{-1}\right)'. \quad (15)$$

Tf denotes the tangent mapping to the mapping $F : x \rightarrow F(x)$, $\mathbb{R}^n \rightarrow \mathbb{R}^n$ i.e. its Jacobian matrix in coordinates. Accordingly T^2F denotes the double tangent, a skew-symmetric bilinear mapping, \mathbb{R}^n -valued, and for any $u \in \mathbb{R}^n$ we define the matrix $D^2F(x)\{u\}$ by $T^2F(u, v) = D^2F(x)\{u\} \cdot v$.

3.3 Innovation

The function In_d , introduced below, is called the innovation. This function reflects the quality measurement of the estimation error on a small moving time interval of size d . The strategy is to adapt the High-gain parameter θ according to In_d . Due to the observability properties of our system, if the \hat{y} is far from y then θ will increase to High-gain mode. Contrarily, if \hat{y} is close to y , the innovation will be small and θ will decrease to 1 (Kalman filtering mode). For this, the variable θ will be subject to the differential equation (19) defined just below.

Let $F_o(\theta)$ be defined as follows:

$$F_o(\theta) = \begin{cases} \frac{1}{\Delta T}\theta^2 & \text{if } \theta \leq \theta_1, \\ \frac{1}{\Delta T}(\theta - 2\theta_1)^2 & \text{if } \theta > \theta_1, \end{cases} \quad (16)$$

where $\theta_1 = \frac{1}{2}\theta_{max}$ and ΔT small enough is a constant. The value θ_{max} depends of the studied system and is obtained by an heuristic approach. It is bounded and the observer remains stable.

The innovation $In_d(t)$, with forgetting horizon d , is:

$$In_d(t) = \int_{t-d}^t \|y(\tau) - \hat{y}(\tau)\|^2 d\tau, \quad (17)$$

where $\hat{y}(\tau)$ is the prediction from the initial state $\hat{x}(t-d)$.

Let us define

$$F(\theta, In_d) = \mu(In_d)F_o(\theta) + (1 - \mu(In_d))\lambda(1 - \theta), \quad (18)$$

for a $\lambda > 0$ and with $\mu(In_d)$ a sigmoid function, $\mu:]-\infty; +\infty[\rightarrow]0; 1[$, $In_d \rightarrow \frac{1}{1+e^{-\beta(In_d-m)}}$. The equation for the HG parameter θ is:

$$\dot{\theta} = F(\theta, In_d). \quad (19)$$

4 APPLICATION

The process under consideration is a real small-size wastewater treatment plant (WWTP) composed of a unique aeration tank equipped with surface aerators which provide oxygen and mix the influent wastewater with biomass (Figure 1).

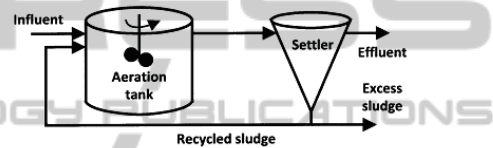


Figure 1: Wastewater treatment plant.

The model used is based upon the Activated Sludge Model N¹ (ASM 1) (Henze et al., 1987). Then the biodegradation model consists of 12 state variables (Table 1). Actually, we consider only biodegradation.

The state variables describing the total alkalinity being not included. The values of stoichiometric and kinetic parameters, as well as the influent concentrations can be found in (Lafont et al., 2011).

The complete set of equations and influent conditions can be found on the International Water Association task group on benchmarking of control strategies for wastewater treatment plants website (<http://www.benchmarkwwtp.org/>, 2011).

The model is of the form $\dot{x} = f(x, u)$, where the control u consists of the state u_b of the turbines and the value Q^{in} of the influent average flow. The input u_b in (20) is a binary sequence switching between 0 and 1 and representing the state of turbines (off/on) that aerate the plant. We make here the reasonable assumptions of three measurements: S_O , S_{NO} and S_{NH} . Although the WWTP with these three outputs is observable, it is too complicated for our purpose. We use a simplified model of lower dimension that has been developed in (Chachuat, 2001).

4.1 The Reduced Model

The author proceeds as follow:

Table 1: List of variables.

Definition	Notation
1. Soluble inert organic matter	S_I
2. Readily biodegradable substrate	S_S
3. Particulate inert organic matter	X_I
4. Slowly biodegradable substrate	X_S
5. Active heterotrophic biomass	$X_{B,H}$
6. Active autotrophic biomass	$X_{B,A}$
7. Particulate products arising from biomass decay	X_P
8. Oxygen	S_O
9. Nitrate and nitrite nitrogen	S_{NO}
10. $NH_4^+ + NH_3$ nitrogen	S_{NH}
11. Soluble biodegradable organic nitrogen	S_{ND}
12. Particulate biodegradable organic nitrogen	X_{ND}

- A single organic compound, denoted X_{DCO} (DCO for “chemical oxygen demand”), is formed by adding soluble and particulate organic compound concentrations $X_{DCO} = S_S + X_S$,

- It is considered that the dynamics of $X_{B,H}$, $X_{B,A}$ and X_{ND} are slow w.r.t. the others.

By removing the three unobservable variables X_P , X_I and S_I , we obtain a simplified model with 5 state variables S_O , S_{NO} , S_{NH} , X_{DCO} and S_{ND} . The three variables S_O , S_{NO} and S_{NH} are observables. All these simplifications provide the following reduced model:

$$\dot{S}_O = \frac{Q^in}{V} (S_O^{in} - S_O) + \alpha_1 \frac{X_{DCO}}{K_{DCO} + X_{DCO}} \cdot \frac{S_O}{K_{O,H} + S_O} + \tilde{r}_1(y) + u_b \cdot k_{La} \cdot (S_O^{max} - S_O) \quad (20)$$

$$\dot{S}_{NO} = \frac{Q^in}{V} (S_{NO}^{in} - S_{NO}) + \alpha_3 \frac{X_{DCO}}{K_{DCO} + X_{DCO}} \cdot \frac{K_{O,H}}{K_{O,H} + S_O} \frac{S_{NO}}{K_{NO} + S_{NO}} + \tilde{r}_2(y) \quad (21)$$

$$\dot{S}_{NH} = \frac{Q^in}{V} (S_{NH}^{in} - S_{NH}) + \alpha_5 \frac{X_{DCO}}{K_{DCO} + X_{DCO}} \cdot \left(\frac{S_O}{K_{O,H} + S_O} + \eta_{NO,g} \frac{K_{O,H}}{K_{O,H} + S_O} \frac{S_{NO}}{K_{NO} + S_{NO}} \right) + \tilde{r}_3(y) + \alpha_6 S_{ND} \quad (22)$$

$$\begin{aligned} \dot{X}_{DCO} = & \frac{Q^in}{V} \left(X_{DCO}^{in} - \frac{K_S}{K_{DCO}} X_{DCO} \right) \\ & + \alpha_7 \frac{X_{DCO}}{K_{DCO} + X_{DCO}} \left(\frac{S_O}{K_{O,H} + S_O} \right. \\ & \left. + \eta_{NO,g} \frac{K_{O,H}}{K_{O,H} + S_O} \frac{S_{NO}}{K_{NO} + S_{NO}} \right) + \alpha_8 \end{aligned} \quad (23)$$

$$\dot{S}_{ND} = \frac{Q^in}{V} (S_{ND}^{in} - S_{ND}) - \alpha_6 S_{ND} + \alpha_9 \cdot \frac{X_{DCO}}{K_{ND} + X_{DCO}} \left(\frac{S_O}{K_{O,H} + S_O} + \eta_{NO,h} \frac{K_{O,H}}{K_{O,H} + S_O} \frac{S_{NO}}{K_{NO} + S_{NO}} \right) \quad (24)$$

$$\begin{aligned} K_{DCO} &= K_S \frac{X_{DCO}}{S_S} \\ K_{ND} &= K_X \frac{X_{DCO}}{X_S} X_{B,H} \end{aligned} \quad (25)$$

$$\begin{aligned} \tilde{r}_1(y) &= \alpha_2 \frac{S_{NH}}{K_{NH,A} + S_{NH}} \frac{S_O}{K_{O,A} + S_O} \\ \tilde{r}_2(y) &= \alpha_4 \frac{S_{NH}}{K_{NH,A} + S_{NH}} \frac{S_O}{K_{O,A} + S_O} \\ \tilde{r}_3(y) &= -\alpha_4 \frac{S_{NH}}{K_{NH,A} + S_{NH}} \frac{S_O}{K_{O,A} + S_O} \end{aligned} \quad (26)$$

The constant k_{La} is the oxygen transfer coefficient ($k_{La} = 10 h^{-1}$) and S_O^{max} is the dissolved oxygen saturation concentration ($S_O^{max} = 8 mg l^{-1}$). The volume of the aeration tank (V) is equal to $6000 m^3$. The settler is a cylindrical tank where the solids are either recirculated to the aeration tank ($Q^{rs} = 18446 m^3 day^{-1}$) or extracted from the system ($Q^w = 385 m^3 day^{-1}$). The parameter values α_1 , α_2 , α_3 , α_4 , α_5 , α_6 , α_7 , α_8 , α_9 , K_{ND} and K_{DCO} are given in Table 2.

4.2 Change of Variables

We apply the developed observer to a simplified model (five states, three outputs). The change of variables Ψ which relates natural coordinates to observer coordinates is trivial. It consists of setting just :

$$\widetilde{X}_{DCO} = \frac{X_{DCO}}{K_{DCO} + X_{DCO}}. \quad (27)$$

The state vector $x = (S_O \ S_{NO} \ S_{NH} \ X_{DCO} \ S_{ND})'$ is changed for $\xi = (S_O \ S_{NO} \ S_{NH} \ \widetilde{X}_{DCO} \ S_{ND})'$, therefore our system is almost naturally in observable coordinates. The inverse Jacobian is trivial to compute.

The choice of parameters for the adaptation of innovation is presented in Table 3.

5 RESULTS

Simulations with the perturbed outputs are carried out by an additive Orstein-Uhlenbeck process. The

Table 2: Constant coefficients.

Coefficient	α_1	α_2	α_3	α_4	α_5	α_6	α_7	α_8	α_9	K_{DCO}	K_{ND}
Value	- 5892	- 875	- 1648	191	- 957	150	- 17855	830	561	574	296

Table 3: Parameters for the adaptation.

Parameter	value
θ_{max}	300
β	$1664 \frac{\pi}{e}$
m	1
ΔT	0.01
λ	200
δ	0.01
d	0.1

alternative control u_b has been chosen: “On” during 15 minutes and “Off” during 5 minutes. The simulations cover 14 days and the value of the input flow rate Q^{in} come from the benchmark file (<http://www.benchmarkwtp.org/>, 2011). We have three files: One for the dry weather, one for the storm weather and one for the rain file.

To evaluate the performances of our observer we have compared an ordinary EKF with our adaptive HG-EKF presented in (Lafont et al., 2011). Considering the obtained results for this system, we propose to use this adaptive HG-EKF observer for the diagnosis.

5.1 Threshold Level for each Output

For each output, we simulate the three files, without fault, to determine the threshold level δ_i (Table 4).

Table 4: Threshold level.

File/Output	S_O	S_{NO}	S_{NH}
Dry	0.2505	0.9453	0.2466
Rain	0.2440	0.9306	0.2247
Storm	0.2576	0.9605	0.2200

We have selected one threshold level by output. For S_O , the taken threshold is 0.3, for S_{NO} , 1.0 and for S_{NH} , 0.3. These levels must be valid for whatever file.

5.2 Faults

The bias and the drift faults are simulated. The bias value is equal to 1.5 and 2. The drift fault is simulated with two curve slopes: $(t - t_f)$ and $2 * (t - t_f)$, t_f is the fault time and t is the simulation time.

Results are presented in Tables 5 and 6 where t_d is the detection time. Only the results for the fault time equal to 3 with the dry file are presented in Table 5. Indeed, the three files have the same seven first days.

Moreover, Tables 5 and 6 present two interesting results:

- Whatever the fault time t_f , the various faults are detected,
- If the fault is more important, it is detected quickly.

6 CONCLUSIONS AND FUTURE WORKS

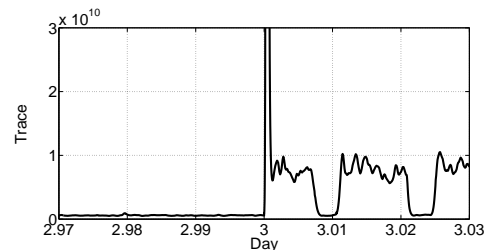
6.1 Conclusions

We have shown that an adaptive HG-EKF observer is efficient to detect sensor faults such as bias and drift. The proposed method imposes to determine the threshold levels with no fault. Thanks to the “robustness” (compared with noise and initial conditions) of this observer and the threshold choice for the residues, the adaptive HG-EKF observer is an interesting approach for the sensor diagnosis. Moreover, the residual generation is very easy.

To improve the method, we can work with the eigenvalues of the matrix p . The calculation of the trace permits to give a confirmation:

$$\text{Trace}(p) = \sum_{i=1}^n V_i, \quad (28)$$

where V_i are the eigenvalues. When there is a sensor fault, the trace has an abrupt change (Figure 2). This result is a complementary information but it is not satisfactory, because if the value Q^{in} increases, the trace becomes very big and the algorithm indicates a false alarm.


 Figure 2: Trace with a fault at $t_d = 3$ days.

6.2 Future Works

To improve this method, we can use the trace properties. The trace value is compared with the influ-

Table 5: Faults detection for the dry file.

Fault/Sensor	S_O	S_{NO}	S_{NH}
	t_d	t_d	t_d
Bias +1.5, $t_f = 3$	3.0002	3.012	3.0004
Bias +1.5, $t_f = 12$	12.0001	12.158	12.0004
Bias +2, $t_f = 3$	3.0001	3.009	3.0003
Bias +2, $t_f = 12$	12.0001	12.028	12.0002
Drift $(t - t_f)$, $t_f = 3$	3.222	4.455	3.215
Drift $(t - t_f)$, $t_f = 12$	12.150	12.739	12.197
Drift $2 * (t - t_f)$, $t_f = 3$	3.092	3.539	3.090
Drift $2 * (t - t_f)$, $t_f = 12$	12.067	12.959	12.115

Table 6: Faults detection for the rain and storm file.

Fault/Sensor	S_O	S_{NO}	S_{NH}	File
	t_d	t_d	t_d	
Bias +1.5, $t_f = 12$	12.0001	12.189	12.0004	Rain
Bias +2, $t_f = 12$	12.0001	12.013	12.0003	
Drift $(t - t_f)$, $t_f = 12$	12.176	13.528	12.189	
Drift $2 * (t - t_f)$, $t_f = 12$	12.086	12.933	12.084	
Bias +1.5, $t_f = 12$	12.0001	12.201	12.0005	Storm
Bias +2, $t_f = 12$	12.0001	12.012	12.0003	
Drift $(t - t_f)$, $t_f = 12$	12.175	13.813	12.203	
Drift $2 * (t - t_f)$, $t_f = 12$	12.089	12.941	12.084	

ent flow rate by developing a “black box” (neural networks for example) which select the peak level to notify a fault.

REFERENCES

Alcaraz-Gonzalez, V., Harmand, J., Rapaport, A., Steyer, J.-P., Gonzalez-Alvarez, V., and Pelayo-Ortiz, C. (2002). Software sensors for highly uncertain wwtps : a new approach based on interval observers. *Water Research*, 36:2515–2524.

Assis, A. and Filho, R. (2000). Soft sensors development for on-line bioreactor state estimation. *Computers and Chemical Engineering*, 24:1099–1103.

Boizot, N., Busvelle, E., and Gauthier, J.-P. (2010). An adaptive high-gain observer for nonlinear systems. *Automatica*, 46:1483–1488.

Chachuat, B. (2001). *Methodology of dynamic optimisation and optimal control of small-size activated sludge wastewater treatment plants*. PhD, Institut National Polytechnique de Lorraine, Nancy.

Dochain, D. (2008). *Bioprocess control*. volume ISBN 9781848210257. ISTE.

Henze, M., Grady, C., Gujer, W., Marais, G., and Matsuo, T. (1987). Activated sludge model n1. In IAWQ, editor, *Technical Report 1*. London.

<http://www.benchmarkwwtp.org/> (2011).

Lafont, F., Busvelle, E., and Gauthier, J.-P. (2011). An adaptive high-gain observer for wastewater treatment systems. *Journal of Process Control*, 21:893–900.

Methnani, S., Gauthier, J.-P., and Lafont, F. (2011). Sensor fault reconstruction and observability for unknown inputs, with an application to wastewater treatment plants. *International Journal of Control*, 84.4:822–833.

Nejjari, F., Puig, V., Giancristofaro, L., and Koehler, S. (July 6-11, 2008). Extended luenberger observer-based fault detection for an activated sludge process. *Proceedings of the 17th World Congress The International Federation of Automatic Control, Seoul, Korea*, pages 9725–9730.

Sotomayor, O., Park, S., and Garcia, C. (2002). Software sensor for on-line estimation of the microbial activity in activated sludge systems. *ISA Transactions*, 41:127–143.